ChemComm

Accepted Manuscript

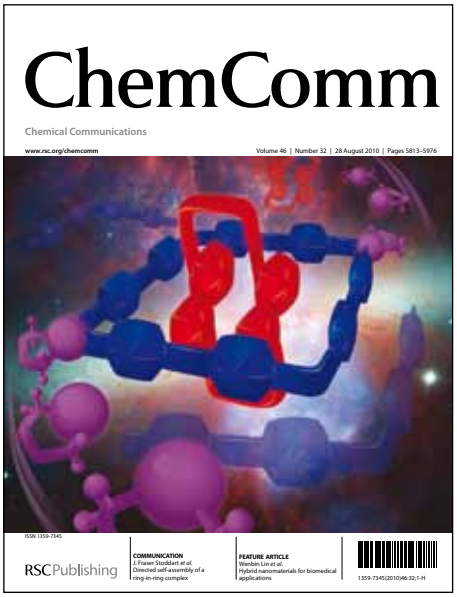

This is an *Accepted Manuscript*, which has been through the RSC Publishing peer review process and has been accepted for publication.

Accepted Manuscripts are published online shortly after acceptance, which is prior to technical editing, formatting and proof reading. This free service from RSC Publishing allows authors to make their results available to the community, in citable form, before publication of the edited article. This *Accepted Manuscript* will be replaced by the edited and formatted *Advance Article* as soon as this is available.

To cite this manuscript please use its permanent Digital Object Identifier (DOI®), which is identical for all formats of publication.

More information about *Accepted Manuscripts* can be found in the **Information for Authors**.

Please note that technical editing may introduce minor changes to the text and/or graphics contained in the manuscript submitted by the author(s) which may alter content, and that the standard **Terms & Conditions** and the **ethical guidelines** that apply to the journal are still applicable. In no event shall the RSC be held responsible for any errors or omissions in these *Accepted Manuscript* manuscripts or any consequences arising from the use of any information contained in them.

Cite this: DOI: 10.1039/c0xx00000x

www.rsc.org/xxxxxx

COMMUNICATION

Coupling of tyrosine deprotonation and axial ligand exchange in nitrocytochrome *c*

Daiana A. Capdevila,[a] Damián Álvarez-Paggi,[a] Maria A. Castro,[a] Verónica Tórtora,[b] Verónica Demicheli,[b] Darío A. Estrín,[a] Rafael Radi,*[b] Daniel H. Murgida*[a]

Received (in XXX, XXX) Xth XXXXXXXXX 20XX, Accepted Xth XXXXXXXXX 20XX
DOI: 10.1039/b000000x

Here we report a spectroscopic, electrochemical and computational study of cytochrome *c* showing that nitration of Tyr74 induces Tyr deprotonation, which is coupled to Met/Lys axial ligand exchange. The structural change results in altered electron shuttling capability and augmented peroxidatic activity of nitrocytochrome *c* at physiological pH.

Ortho-nitration of tyrosine residues is a post-translational modification that has been reported for a variety of proteins under basal physiological conditions, and that is significantly augmented under diverse pathological conditions.[1] The accepted mechanism of nitration involves one-electron oxidation of Tyr to Tyr$^{\bullet}$ followed by reactions with either $^{\bullet}$NO or $^{\bullet}NO_2$, resulting in $^{\bullet}$NO-dependent oxidative modifications. The size and electron withdrawing characteristics of the $-NO_2$ substituent are likely to perturb structural and electronic features of the protein that may result in decreased or increased activity, as well as in the gain of a new function.[2] Unveiling the mechanisms of functional modulation is crucial for a number of physiological and/or pathological conditions.

Here we report on the molecular mechanism underlying loss of electron shuttling capability and concomitant gain of peroxidatic activity of horse heart cytochrome *c* (Cyt) upon tyrosine nitration. Cyt is a 12 kD soluble monohemic protein present at mM levels in the mitochondrial intermembrane space,[3] whose primary function is transporting electrons from complex III to the terminal O_2-reductase in the respiratory electron transport chain. Specific and unspecific electrostatic interactions of Cyt with negatively charged counterparts have been extensively studied and found to be determinant for the optimization of electron transfer parameters such as electronic coupling and reorganization energy,[4-7] as well as for inducing structural changes.[8-14] Specifically, it has been proposed that Cyt/cardiolipin interactions lead to structural changes at the level of the heme pocket that include detachment of the iron axial ligand Met80 and, eventually, to its replacement by either a lysine or a histidine residue.[8-13] The first case resembles the so-called alkaline transition.[15] The alternatively ligated isomers of Cyt present increased peroxidatic activity against cardiolipin, suggesting a role in mitochondrial membrane permeabilization during the early events of apoptosis.

Mammalian Cyt contains four highly conserved Tyr residues at sequence positions 48, 67, 74 and 97. Treatment with peroxynitrite leads to preferential mononitration of either Tyr74 or Tyr97 which, in contrast to residues 48 and 67, are solvent exposed.[16] These modifications have been reported to result in early alkaline transitions with apparent pK_a^{alk} values of 7.3 and 8.7, respectively that contrast with the value of 9.4 determined for unmodified Cyt.[15;17] NMR experiments confirmed that in all cases the transition implies replacement of Met80 by a Lys residue as axial ligand. Based on these results, it has been proposed that nitration of Tyr74 may be implicated in oxidative sensing and signalling of apoptosis via oxidation of cardiolipin and other mitochondrial targets. Moreover, it has been speculated that the conformational transition does not involve deprotonation of the nitrated Tyr but, instead, is driven by steric perturbations of the flexible Ω loop comprising residues 70-85.[17] While a plausible hypothesis, the molecular mechanism by which nitration of a solvent exposed residue elicits an early alkaline transition remains to be elucidated. For this purpose we performed acid-base titrations of ferric WT Cyt and of the mononitrated variants at positions 74 (NO_2-Cyt_{74}) and 97 (NO_2-Cyt_{97}) using UV-Vis absorption and resonance Raman (RR) detection. In the first case the evolution of the alkaline transition is determined from the disappearance of the charge transfer band at 695 nm (Figure S3). RR titrations performed under Soret excitation (413 nm laser line) are much more informative as the marker band region (*ca.* 1300-1700 cm^{-1}) is highly sensitive to the redox state, spin and axial ligands of the heme iron.[13;18-21] Figure 1 displays typical RR spectra obtained at different pH values.

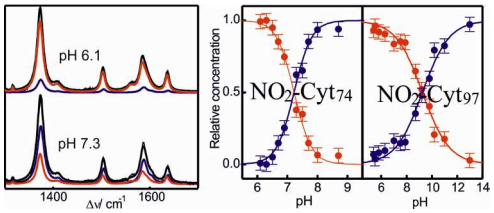

Figure 1. Left: RR spectra of ferric NO_2-Cyt_{74} recorded at different pH values (λ_{ex} = 413 nm). Black: experimental spectra. Red: native spectral component. Blue: alkaline spectral component. Right: Relative concentrations of the native (red) and alkaline (blue) isomers of NO_2-Cyt_{74} and NO_2-Cyt_{97} as a function of pH, as determined by RR.

The spectral sets for the three protein variants (WT, NO_2-Cyt_{74} and NO_2-Cyt_{97}) can be quantitatively simulated with varying

proportions of only two spectral components: (i) native low spin ferric Cyt with a Met/His axial coordination pattern and (ii) an alkaline form characterized by a low spin ferric heme with Lys/His axial coordination.[20;21]

Table 1. Reduction potentials and pK_a values of Cyt variants.

Species	[a] pK_a^{alk}	[b] pK_a^{alk}	[c] pK_a^{Tyr}	E^0_{native} (mV)	E^0_{alk} (mV)
WT	9.4± 0.1	9.4 ± 0.1	N.D.	[d]254 ± 5	[d]-148 ± 5
NO_2-Cyt$_{97}$	9.2± 0.2	9.4 ± 0.1	6.2 ± 0.1	[d]247 ± 9	[d]-161 ± 7
NO_2-Cyt$_{74}$	7.0± 0.1	7.1 ± 0.1	7.1 ± 0.1	[d]N.D.	[d]-173 ± 5
				[e]263 ± 5	[e]-132 ± 5

[a]UV-Vis at 695nm [b]RR at 413 nm. [c]RR at 458 nm. [d]pH 7. [e]pH 10.

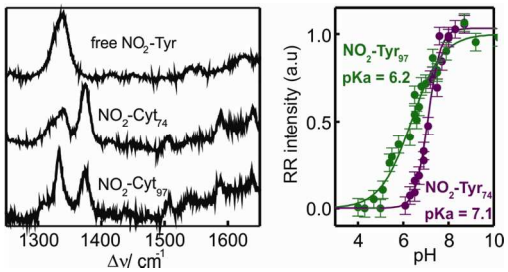

Figure 2. Left: RR spectra of free NO_2-Tyr, NO_2-Cyt$_{74}$ and NO_2-Cyt$_{97}$ at pH 9 (λ_{exc} = 458 nm). Right: normalized RR intensity of deprotonated NO_2-Tyr in NO_2-Cyt$_{97}$ (green) and NO_2-Cyt$_{74}$ (purple) as a function of the solution pH. See ESI for further details.

Quantification of the two species by spectral component analysis allows determining the pK_a^{alk} values for the alkaline transition in each case (Figure 1 and Table 1). RR titrations provide conclusive evidence that nitration of Tyr97 has no effect on the alkaline transition of Cyt, ruling out a mild effect suggested by previous titrations.[17] The small discrepancy is mainly ascribed to the larger error and lack of specificity of the UV-Vis titration that is solely based on the disappearance of a very weak absorption band that in the case of NO_2-Cyt$_{97}$ is even weaker. Nitration of Tyr74, on the other hand, results in a two units downshift of the pK_a^{alk} that is consistently reproduced by RR and UV-Vis titrations. In good agreement with previous NMR determinations,[17] the RR experiments indicate that the neutral and alkaline forms are similar in the three protein variants in terms of coordination pattern and coarse structural features at the level of the heme pocket. Consistently, cyclic voltammetry experiments in solution (Figure S4) afford similar reduction potentials for the corresponding Met/His and Lys/His forms of the three protein variants, which in average are 255 and -161 mV, respectively (Table 1), thus underlying the loss of electron transport capability upon ligand exchange.

The acid-base equilibrium of free NO_2-Tyr in aqueous solution can be easily monitored by UV-Vis absorption given that the acidic and basic forms of the nitrophenolic group present well separated maxima at 357 and 426 nm, respectively, and an isosbestic point at 379 nm, yielding pK_a^{Tyr} = 6.8 ± 0.1 (Figure S5). An almost identical value (pK_a^{Tyr} = 6.9 ± 0.1) is obtained by monitoring the RR intensity of the basic form as a function of pH recorded under 458 nm excitation. For NO_2-Cyt UV-Vis titrations are hampered by the strong overlap of the weak bands of the nitrated residue with the strong absorption of the heme. RR spectra obtained with 458 nm, on the other hand, display well resolved vibrational bands of the heme group and of the basic form of the NO_2-Tyr residue with comparable intensities, thereby allowing for reliable simultaneous titrations of the two chromophores in the proteins (Figure 2). As summarized in Table 1, the pKa value determined for NO_2-Tyr97 is somewhat lower than for free NO_2-Tyr in aqueous solution indicating that, in spite of being a surface residue, the environment is slightly different, probably due to partial burial into the protein matrix. For NO_2-Tyr74, on the other hand, the pK_a^{Tyr} is identical within error to the free NO_2-Tyr in aqueous solution, thus suggesting full exposure of this residue to the solvent. Based on these observations, one might expect larger perturbations of the protein structure upon nitration of Tyr97 compared to Tyr74, leading to a more pronounced labilization of the MetS-Fe bond that favours an earlier alkaline transition in the first case. The experimental results, however, contradict this idea. Moreover, while the alkaline transition and NO_2-Tyr deprotonation appears to be completely decoupled for NO_2-Cyt$_{97}$, the p*Ka* values of both processes are identical for NO_2-Cyt$_{74}$, thus suggesting that Lys/Met ligand exchange is triggered by electrostatic perturbation of the protein structure upon NO_2-Tyr74 deprotonation. To gain deeper insight into these processes we performed molecular dynamics (MD) simulations (see ESI for details). Root mean square deviations of both Tyr74-protonated and deprotonated NO_2-Cyt$_{74}$ with respect to the WT protein are very small, typically below 0.7 Å. Consistently, secondary structure elements as determined from the MD simulations show only subtle alterations (Figures S6-S7). Steered MD (SMD) simulations, on the other hand, show that the free energy change for displacing the axial ligand Met80 is essentially identical for WT and both the (NO_2-Tyr74)-protonated and deprotonated forms NO_2-Cyt$_{74}$ (Figure 3).

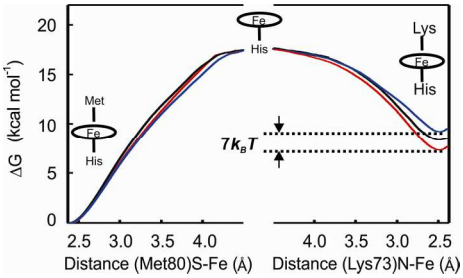

Figure 3. Free energy for displacing Met80 (left) and Lys73 (right) in the native and alkaline isomers, as estimated by SMD. Black: non-nitrated Cyt. Blue: protonated NO_2-Cyt$_{74}$. Red: deprotonated NO_2-Cyt$_{74}$.

As the 3D structure of the alkaline isomer of horse heart Cyt is not available, we created *in silico* models starting from the NMR structure of alkaline iso-Cyt in which the sixth axial ligand is Lys73 (see ESI for details).[22] SMD simulations performed on the model structures show that the free energy required for pulling the Lys73 ligand apart from the iron increases in the order protonated NO_2-Cyt$_{74}$ < WT < deprotonated NO_2-Cyt$_{74}$, where the protonation state refers to the NO_2-Tyr74 phenolic group.

The alkaline transition of Cyt is a complex process that involves several steps, some of them common to the folding/unfolding pathway. Stopped-flow and NMR experiments suggest that the crucial events are partial unfolding of the Ω loop 40-57 that leads to deprotonation of an unidentified internal group, followed by the Met/Lys ligand exchange reaction itself. The last step has

been identified as rate limiting and requires deprotonation of the ligating surface Lys residue (pKa_{Lys} = 11.4) and rearrangement of the Ω loop 70-85.[23-26] The equilibrium reaction can be described in terms of a minimal model:

$$\text{Cyt-H}_{(\text{Met-Fe})} \overset{pKa = 11.4}{\rightleftharpoons} \text{Cyt}_{(\text{Met-Fe})} \underset{k_b}{\overset{k_f}{\rightleftharpoons}} \text{Cyt}_{(\text{Lys-Fe})} \quad \text{(Scheme 1)}$$

which leads to the expression $pK_a^{alk} = 11.4 - \log(k_f / k_b)$, with $k_f \approx 7.5\ s^{-1}$ and $k_b \approx 0.02\ s^{-1}$.[26] Assuming that the rate constant of the back alternative ligation reaction (k_b) is determined by the activation barrier for breaking the Lys-Fe bond, a simple Eyring-type calculation based on the results presented in Figure 3 anticipates a 6-fold decrease of k_b for (NO_2-Tyr74)-deprotonated NO_2-Cyt_{74} compared to the non-nitrated protein. Assuming that k_f is not significantly affected by Tyr nitration this yields $pK_a^{alk} \approx 8$ for NO_2-Cyt_{74}, which considering the approximations involved, is in reasonable agreement with the experimental value. Thus, the present experimental and computational results suggest that the early alkaline transition in NO_2-Cyt_{74} arises from stabilization of the alkaline isomer by the deprotonated NO_2-Tyr74 residue rather than by destabilisation of the native form. Note that for the alkaline isomer containing protonated NO_2-Tyr74 the activation barrier for displacing the ligating Lys is lower than for the deprotonated form by approximately 7 times the thermal energy at room temperature ($7k_BT$), thereby suggesting significant protein destabilization (and up-shift of pK_a^{alk}) upon protonation.

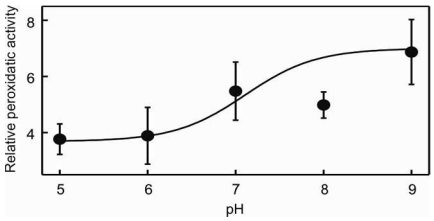

Figure 4. Peroxidatic activity of NO_2-Cyt_{74} relative to WT-Cyt, as a function of pH determined by amplex red assay. The line was drawn using the parameters determined in Figures 1 and 2 for NO_2-Cyt_{74}.

For the minimal model shown in Scheme 1 the acid-base equilibrium with apparent p*Ka* = 11.4 has been assigned to the deprotonation of Lys73 and/or 79. While Lys deprotonation is clearly required for coordination to the heme iron, the high value of the apparent p*Ka* underlines a more complex scheme that might include deprotonation of Tyr74 as crucial event, as suggested by the identity of the pK_a^{Tyr} and pK_a^{alk} values determined here for NO_2-Cyt_{74}. Independently of the detailed mechanism, we observe a one-to-one correlation between NO_2-Tyr74 deprotonation, alkaline transition and increase of peroxidatic activity relative to WT Cyt (see Figure 4 and ESI).

In summary, the present results demonstrate that nitration of Tyr74 in Cyt induces deprotonation of this residue concomitant with the so-called "alkaline transition" at neutral pH. The effect is ascribed to the stabilization of the alkaline form by the deprotonated NO_2-Tyr74, and results in a *ca.* 7-fold increase of the peroxidatic activity and in the loss of electron shuttling function due to a *ca.* 400 mV downshift of the reduction potential. The pH in the intermembrane space is typically 6.8, and it becomes only slightly more acidic under apoptotic signalling.[27] Thus, a significant proportion of the alternative conformation of NO_2-Cyt_{74} can be expected at any biologically-relevant pH.

We thank ANPCyT, UBACyT, CONICET, CeBEM, ANII, CSIC-UdelaR and NIH for financial support, and Dr. Batthyany for his advice on MS. Simulations were performed using the Open Science Grid supported by the NSF and the U.S. Department of Energy´s Office of Science.

Notes and references

[a] *Departamento de Química Inorgánica, Analítica y Química Física and INQUIMAE, Facultad de Ciencias Exactas y Naturales, Universidad de Buenos Aires-CONICET, Argentina. E-mail: dhmurgida@qi.fcen.uba.ar*
[b] *Departamento de Bioquímica and Center for Free Radical and Biomedical Research, Facultad de Medicina, Universidad de la República, Montevideo, Uruguay. E-mail: rradi@fmed.edu.uy*

†Electronic Supplementary Information (ESI) available: experimental procedures, UV-Vis and RR titrations, voltammetries, structural models. See DOI: 10.1039/b000000x/

1. R. Radi, *Acc. Chem. Res*., 2013, **46**, 550.
2. J. M. Souza, G. Peluffo, and R. Radi, *Free Rad. Biol. Med*., 2008, **45**, 357.
3. H. J. Forman and A. Azzi, *FASEB J*., 1997, **11**, 374.
4. D. Alvarez-Paggi, M. A. Castro, V. Tortora, L. Castro, R. Radi, and D. H. Murgida, *J. Am. Chem. Soc*., 2013, **135**, 4389.
5. D. Alvarez-Paggi, D. F. Martin, P. M. DeBiase, P. Hildebrandt, M. A. Marti, and D. H. Murgida, *J. Am. Chem. Soc*., 2010, **132**, 5769.
6. S. Monari, A. Ranieri, C. A. Bortolotti, S. Peressini, C. Tavagnacco, and M. Borsari, *Electrochim.Acta*, 2011, **56**, 6925.
7. G. Battistuzzi, M. Borsari, C. A. Bortolotti, G. Di Rocco, A. Ranieri, and M. Sola, *J. Phys. Chem. B*, 2007, **111**, 10281.
8. G. Balakrishnan, Y. Hu, O. F. Oyerinde, J. Su, J. T. Groves, and T. G. Spiro, *J. Am. Chem. Soc.*, 2007, **129**, 504.
9. J. M. Bradley, G. Silkstone, M. T. Wilson, M. R. Cheesman, and J. N. Butt, *J. Am. Chem. Soc.*, 2011, **133**, 19676.
10. J. Hanske, J. R. Toffey, A. M. Morenz, A. J. Bonilla, K. H. Schiavoni, and E. V. Pletneva, *Proc. Nat. Acad. Sci. USA*, 2012, **109**, 125.
11. V. E. Kagan, H. A. Bayir, N. A. Belikova, O. Kapralov, Y. Y. Tyurina, V. A. Tyurin, J. F. Jiang, D. A. Stoyanovsky, P. Wipf, P. M. Kochanek, J. S. Greenberger, B. Pitt, A. A. Shvedova, and G. Borisenko, *Free Rad. Biol. Med.*, 2009, **46**, 1439.
12. Y. L. P. Ow, D. R. Green, Z. Hao, and T. W. Mak, *Nature Rev. Mol. Cell Biol.*, 2008, **9**, 532.
13. F. Sinibaldi, B. D. Howes, E. Droghetti, F. Polticelli, M. C. Piro, D. Di Pierro, L. Fiorucci, M. Coletta, G. Smulevich, and R. Santucci, *Biochemistry*, 2013, **52**, 4578.
14. H. Wackerbarth, D. H. Murgida, S. Oellerich, S. Dopner, L. Rivas, and P. Hildebrandt, *J. Mol. Str.*, 2001, **563**, 51.
15. S. I. Rosell, J. C. Ferrer, and A. G. Mauk, *J.Am.Chem.Soc*., 1998, **120**, 11234.
16. J. M. Souza, L. Castro, A. M. Cassina, C. Batthyany, and R. Radi, *Methods Enzymol*., 2008, **441**, 197.
17. L. A. Abriata, A. Cassina, V. Tortora, M. Marin, J. M. Souza, L. Castro, A. J. Vila, and R. Radi, *J. Biol. Chem.*, 2009, **284**, 17.
18. D. H. Murgida and P. Hildebrandt, *Acc. Chem. Res*., 2004, **37**, 854.
19. G. Balakrishnan, Y. Hu, O. F. Oyerinde, J. Su, J. T. Groves, and T. G. Spiro, *J. Am. Chem. Soc.*, 2007, **129**, 504.
20. S. Dopner, P. Hildebrandt, F. I. Rosell, and A. G. Mauk, *J. Am. Chem. Soc.*, 1998, **120**, 11246.
21. S. Dopner, P. Hildebrandt, A. G. Mauk, H. Lenk, and W. Stempfle, *Spectrochim. Acta A*, 1996, **52**, 573.
22. M. Assfalg, I. Bertini, A. Dolfi, P. Turano, A. G. Mauk, F. I. Rosell, and H. B. Gray, *J. Am. Chem. Soc.*, 2003, **125**, 2913.
23. S. Bandi and B. E. Bowler, *Biochemistry*, 2011, **50**, 10027.
24. P. Weinkam, J. Zimmermann, L. B. Sagle, S. Matsuda, P. E. Dawson, P. G. Wolynes, and F. E. Romesberg, *Biochemistry*, 2008, **47**, 13470.
25. T. D. Perroud, M. P. Bokoch, and R. N. Zare, *Proc. Nat. Acad. Sci. USA*, 2005, **102**, 17570.
26. L. Hoang, H. Maity, M. M. G. Krishna, Y. Lin, and S. W. Englander, *J. Mol. Biol.*, 2003, **331**, 37.
27. J. Santo-Domingo and N. Demaurex, *J.Gen.Physiol*., 2012, **139**, 415.